Lattice Occupied Voxel Lists for Representation of Spatial Occupancy

Julian Ryde and Michael Brünig

Abstract— The characteristics of a variety of 3D lattices are assessed for their performance when applied to typical robotics problems. The lattices studied are the Cubic, Body Centred Cubic (BCC), Face Centred Cubic (FCC), hexagonal prismatic and finally the Mean Centred Cuboidal (MCC). An algorithm for generic quantization to any low dimensional lattice is presented allowing this analysis to be easily extended to other 3D lattices of interest.

Tests are undertaken on uniform sampled random data and laser range data from mobile robot platforms including an autonomous skid steer loader. The improvements in accuracy, memory requirements and consistency under rotation for the alternative lattices over the cubic lattice are typically 5-10%.

The radial distribution of lattice points is studied through the distribution of points assigned to the same lattice cell and that in neighbouring cells. For instance only 12 neighbouring cells need checking for the FCC lattice as opposed to the cubic lattice which requires 26. Not only are fewer checks required but the distance variation associated with points in adjacent voxels of the FCC lattice is substantially lower than that of a cubic lattice. For the FCC lattice these point distances have a 30% smaller standard deviation and a 40% smaller range. These results make algorithms, such as collision checking and scan/map matching, which often involve many proximity checks, significantly faster and more accurate.

I. INTRODUCTION

Many algorithms employed in robotics use quantization. Indeed in a manner of speaking all data is quantized or digitised once it is represented internally to a computer. Due to memory and processor limitations quantization at a coarser level is often done, for example occupancy grids [1]–[3] representing 2D maps and occupied voxel lists [4] for 3D maps.

The theory behind the lattice quantization approaches has been thoroughly investigated for vector quantization and extensive literature is available, [5]–[8].

Occupied voxel lists are similar to occupancy grids, however the important difference is that they are a list containing only those voxels that have been observed to be occupied, rather than a grid structure containing the occupancy of all voxels. It is done in this manner because 2D occupancy grids do not scale well to 3D, consuming an inordinate amount of memory. For both occupancy grids and occupied voxel lists incoming data points from sensors have to be assigned to the appropriate cells in a process referred to as quantization. Occupancy voxel lists are a compact and efficient (in terms of update and query) representation suitable for visualisation, SLAM, localisation, point cloud alignment and collision avoidance. Although the occupied voxel lists do not intrinsically differentiate between unoccupied cells and

Authors are with the Autonomous Systems Laboratory, CSIRO ICT Centre, Brisbane, Australia `julian.ryde@csiro.au`

those that have yet to be observed, as discussed in [9] such information can be generated from an occupied voxel list map and the associated robot poses used to build the map. Alternatively the free space voxels can be also stored as a voxel list, probably at a coarser resolution due to memory constraints.

One of the advantages of the alternative lattices presented here is that they are compatible with existing algorithms, such as iterative closest point (ICP), and data structures [9]. In this vein occupied voxel lists have been combined with the procedures for quantizing to non-cubic lattices.

Once the process of converting from continuous data to the corresponding nearest discrete lattice points has been implemented the quantized lattice points can then be processed by other algorithms. In the case of ICP the alignment of two scans may be simply carried out on the quantized lattice points rather than the raw point clouds. There are advantages for doing this, namely a reduction in the number of points that need processing if there are many points in close proximity to each other, and the possibility of filtering erroneous points.

The quantization error, alternatively known as the distortion, is an illuminating metric and consequently its variation with 3D rotation assessed in this paper. We also present voxel count distributions, which are indicative of the storage required for the occupied voxel list. This testing is done on both random and real 3D laser range data.

From these experiments it is evident that there is a consistent improvement in terms of accuracy, reliability and consistency under rotation of the FCC lattice over the conventional cubic lattice.

This builds upon the investigation undertaken in [10], specifically by developing a more general lattice quantization algorithm that works for all low dimensional lattices. This enables the testing of numerous 3D lattices such as cubic, FCC, BCC, MCC and hexagonal prismatic. The mean centred cuboid lattice is presented, tested and its Voronoi cell shown. These lattices are tested with both random points and actual data from a robot (Fig. 2) to ascertain their performance with full 6DOF trajectory and map data. Additionally, the pose accuracy of 3D laser scan matching with the different lattices is presented.

Finally an analysis of the adjacent voxels for each lattice is undertaken. This is of interest because given an occupied voxel list of an operating arena, not only might one need to know whether a given voxel is unoccupied but it is also necessary to know if any of the adjacent voxels are occupied. Two points could be very close but be in different voxels because they lie either side of a voxel boundary. However,
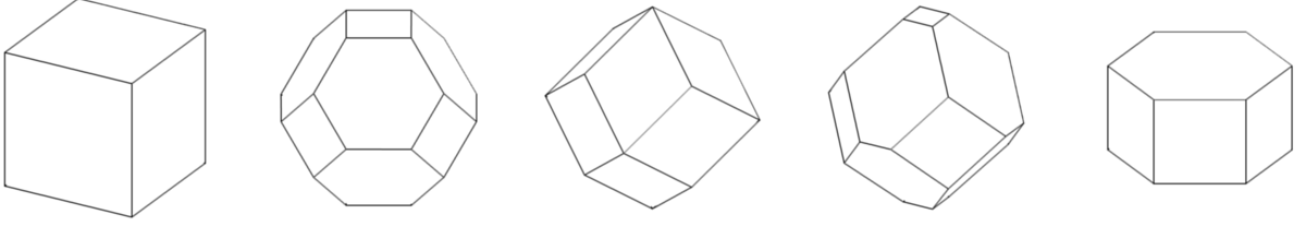
Fig. 1. Voronoi cells for the lattices cubic, body centred cubic (BCC), face centred cubic (FCC), mean centred cuboidal (MCC) and hexagonal prismatic. The polyhedra are cube, truncated octahedron, rhombic dodecahedron, MCC Voronoi cell and hexgonal prism.

for some queries we need to know that there is at least some minimum clearance such as collision avoidance, path planning and scan matching.

Section II provides background to the lattices studied and the methods for quantizing data to them. A brief description of the experiments performed and the experimental method are contained in Section III. The results from these experiments and the discussion of them is combined into Section IV. Finally the paper is concluded in Section V.

II. GENERIC LOW DIMENSIONAL LATTICE QUANTIZATION

The NP-hard nature of the closest lattice point problem is widely discussed [11], [12] and such lattice problems have even been suggested for cryptographic purpose [13]. However for low dimensions quantization to an arbitrary lattice is practical. Consider the lattice Λ with basis vectors encapsulated in the generator matrix $\mathbf{G}$. For a vector of lattice indices $\vec{w}$ the Cartesian position vector, $\vec{x}$, is defined $\vec{x} = \mathbf{G}\vec{w}$, conversely if $\vec{x}$ is coincident with a lattice point then the integer indices of the lattice point may be determined thus, $\vec{w} = \mathbf{G}^{-1}\vec{x}$.

For the nearest lattice point problem it might seem possible to calculate the nearest lattice point as

$$\vec{\hat{w}} = \lfloor \mathbf{G}^{-1}\vec{x} \rceil \tag{1}$$

with $\lfloor \vec{x} \rceil$ returning the nearest integer to $\vec{x}$.

This however is incorrect and results in the indices being 'off-by-one' in one or more dimensions [10]. An extension to this provides the correct result. The distances from $\vec{x}$ to the lattice point obtained through (1) as well as adjacent lattice points to this are calculated and the minimum selected. This minimum distance corresponds to the lattice point nearest to $\vec{x}$.

If the matrix of off-by-one vectors for the lattice in question is Δ then the generic quantization algorithm is

$$Q(\vec{x}) = \operatorname*{argmin}_{i} \left(\left\| \mathbf{G} \cdot \left(\vec{\hat{w}} + \Delta_i \right) - \vec{x} \right\| \right). \tag{2}$$

The generic low dimensional algorithm summarised in (2) is much faster than a complete search over a restricted lattice but is still slower than algorithms developed for specific lattices [14], [15]. Its advantage is that it works for any lattice basis in low dimensions such as 2D and 3D.

The lattice displacement vectors for the adjacent voxels relative to a given voxel are presented here for a number of 3D lattices.

$$\Delta_{\text{cubic}} = \begin{bmatrix} -1 & -1 & -1 & -1 & & 1 \\ -1 & -1 & -1 & 0 & \dots & 1 \\ -1 & 0 & 1 & -1 & & 1 \end{bmatrix} \tag{3}$$

$$\Delta_{\text{fcc}} = \pm \begin{bmatrix} 1 & 0 & 1 & 0 & 0 & 1 \\ -2 & -1 & -1 & 0 & -1 & -1 \\ -1 & -1 & -1 & -1 & 0 & 0 \end{bmatrix} \tag{4}$$

$$\Delta_{\text{bcc}} = \pm \begin{bmatrix} 1 & 0 & 1 & 0 & 1 & 0 & -1 \\ 1 & 0 & 0 & 1 & 1 & -1 & 0 \\ -2 & -1 & -1 & -1 & -1 & 0 & 0 \end{bmatrix} \tag{5}$$

$$\Delta_{\text{mcc}} = \pm \begin{bmatrix} -1 & 0 & -1 & 0 & -1 & 0 & -1 \\ -1 & -1 & 0 & 0 & -1 & -1 & 0 \\ -1 & -1 & -1 & -1 & 0 & 0 & 0 \end{bmatrix} \tag{6}$$

$$\Delta_{\text{hex}} = \pm \begin{bmatrix} 0 & -1 & 0 & 1 & 0 & 1 & -1 & 0 & -1 \\ -1 & 0 & 0 & 0 & 1 & 1 & -1 & -1 & 0 \\ -1 & -1 & -1 & -1 & -1 & -1 & 0 & 0 & 0 \end{bmatrix} \tag{7}$$

A. Candidate Lattices

Equipped with the generic quantization (2) and given the generator matrix, quantization to a wide variety of interesting 3D lattices can be tested.

The Voronoi cells for each of the lattices are rendered in Fig. 1. The Voronoi cell is the polyhedron that contains the volume associated with each lattice point. If these polyhedra were placed with their centres at the lattice points then the resulting structure would be space filling. These interesting lattices have various properties that make them worthy of consideration and are listed below. The normalised (unit determinant) generator matrix is listed for each lattice.

1) Simple Cubic, Cubic: The simple cubic lattice is the most straightforward lattice that is conventionally used in robotics and other fields.

$$\mathbf{G}_{\text{cubic}} = \begin{pmatrix} 1 & 0 & 0 \\ 0 & 1 & 0 \\ 0 & 0 & 1 \end{pmatrix} \tag{8}$$

2) Body Centred Cubic, BCC: This lattice can be envisaged as a standard cubic lattice with an additional lattice point situated at the body centre of each cube.

$$\mathbf{G}_{\text{BCC}} = \begin{pmatrix} 1.2599 & 0 & 0.6300 \\ 0 & 1.2599 & 0.6300 \\ 0 & 0 & 0.6300 \end{pmatrix} \quad (9)$$

3) Face Centred Cubic, FCC: This can be visualised in a similar manner to the BCC lattice but instead of the extra body centre point there are additional points at the centre of each of the six faces.

$$\mathbf{G}_{\text{FCC}} = \begin{pmatrix} 1.5874 & 0.7937 & 0 \\ 0 & -0.7937 & 0.7937 \\ 0 & 0 & -0.7937 \end{pmatrix} \quad (10)$$

4) Mean Centred Cuboidal, MCC: Recently proved to be an optimal quantizer in [16] this lattice has the characteristic of being isodual [17] in that it is congruent to its dual or reciprocal lattice. It can be thought of as a hybrid of the BCC and FCC lattices.

$$\mathbf{G}_{\text{MCC}} = \begin{pmatrix} 1.0987 & -0.4551 & -0.1885 \\ 0 & 1 & -0.5858 \\ 0 & 0 & 0.9102 \end{pmatrix} \quad (11)$$

5) Hexagonal prismatic, Hex: This lattice is a 2D hexagonal lattice that is extended to 3D as a hexagonal prism. The lattice is considered because of the nature of the environment in which most robots are operating. Most environments have a definite up and down direction defined by the local gravity vector. This influences the structure of the environment and resulting data received by robot sensors. The local gravity is readily determined via an accelerometer when stationary. Thus data such as maps can be appropriately aligned vertically with a lattice in a global coordinate frame. Therefore, rotational invariance is only required about axes aligned with the local gravity for which the hexagonal prismatic lattice is suitable.

$$\mathbf{G}_{\text{Hex}} = \begin{pmatrix} 1.1776 & -0.5888 & 0 \\ 0 & 1.0198 & 0 \\ 0 & 0 & 0.8327 \end{pmatrix} \quad (12)$$

B. Lattice Characteristics

In an effort to ensure fair comparisons between the lattices it is important to normalise the size of the lattice voxels. This is because in order to fully cover all space with the lattice map the maximum number of voxels required is the volume of the space over the primitive unit cell volume. This analysis neglects the edge effects.

For an arbitrary basis defined by the generator matrix $\mathbf{G}$ the primitive cell volume is the volume of the parallelepiped defined by the basis vectors. This volume is given by the determinant of $\mathbf{G}$ and is equal to the Voronoi cell volume.

Another characteristic of a lattice is the distortion as a result of quantizing to the lattice which is defined as

$$E = \tfrac{1}{n} \sum_i \|Q(\vec{x}_i) - \vec{x}_i\|, \quad (13)$$

with $Q(\vec{x})$ a general lattice quantization function, as in (2), and $\vec{x}_i$ the position vector of the ith data point from n such points. The voxel count is the number of unique tuples after quantization and corresponds to the number of lattice points that have at least one data point in their Voronoi cell.

III. EXPERIMENTS

Two main experiments are performed. The first establishes that the predicted desirable properties are in fact present in the data from single 3D scans. These scans are typical of ones acquired on mobile robotic platforms from rotating 2D laser scanners, 2D laser scanners with external rotating mirrors, 3D laser scanners and flash light detection and ranging (LIDAR) systems. The common aspect to all these sensors is that they deliver range data over some field of view which can be represented as a point cloud. Any data structure that this point cloud is converted to should have certain desired properties, such as rotational invariance, accurate representation of the raw data, lower storage requirements and good computational performance. The computational requirements include fast conversion from the raw data format and efficient support of operations that will be typically performed on the data structure.

The second experiment tests the performance of mapping with the various lattices. The lattices tested are simple cubic, the body centred cubic (BCC) and the face centred cubic (FCC). The mapping algorithm is a based on multi-resolution occupied voxel lists [9].

A. Uniform Random Rotations

As the fairness of the comparisons depends on uniformly distributed random 3D rotations some discussion is given to ensuring this is done correctly, [18], [19]. The need for uniform random sampling is also appreciated by other robotics researchers [20]–[22]. In this work we generate random rotation matrices with the method described by [18]. The example scan data is rotated randomly in 3D by application of random rotation matrices before quantizing to the various lattices. The same sample of random rotation matrices is used for each lattice type. In this way a fair test of the lattices is performed without biasing due to the rotational and translational symmetries present resulting from the interaction between the structure of the environment and the lattice patterns.

B. Skid steer loader (Bobcat)

Experiments are also conducted on the platform depicted in Fig. 2 which is suitable for testing the performance of the lattice quantizers under 6DOF pose changes. This platform is equipped with numerous sensors however the ones relevant to the experiments conducted are three laser range finders, one of which is continuously rotating, and an INS/GPS. The laser range finders are standard SICK LMS 200's and the INS/GPS is a Novatel SPAN-CPT combined GPS and inertial navigation solution capable of providing 6DOF pose (position and attitude) at 100Hz. A position error of 0.03m is observed with RTK GPS.

Fig. 2. Autonomous skid steer loader performing an earth moving task. Laser data from both the side lasers and top rotating laser scanner are combined into occupied voxel list maps based on various lattices.
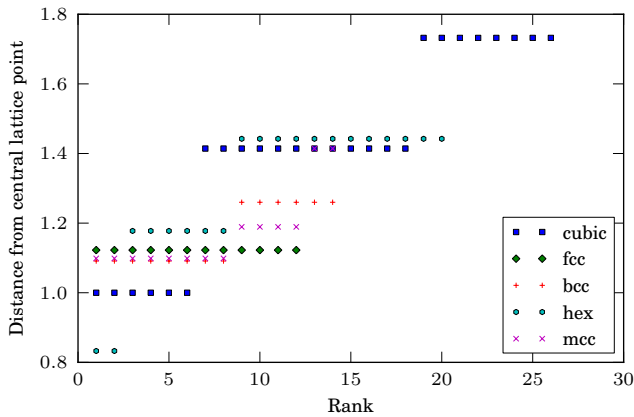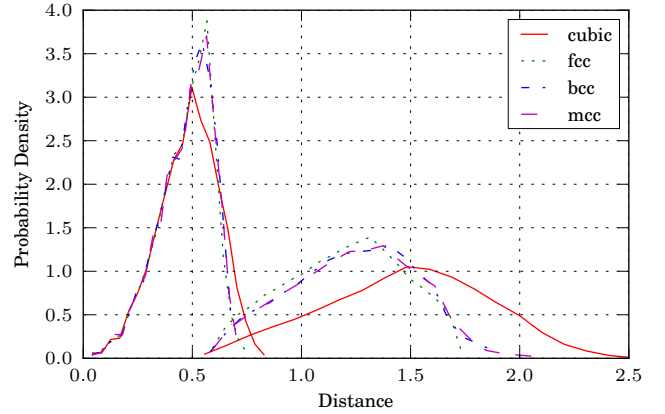

Fig. 4. Distribution of point distances from the Voronoi cell centre for points uniformly sampled across a normalized single cell volume (first set of peaks) and for points in adjacent cells (second set).

Fig. 3. The ordered distances of lattice points from the central lattice point. Each lattice has its curve terminated after the first layer which corresponds to only adjacent voxels.

The pose from the INS is used to transform the laser range returns, measured in the coordinate frame of the robot into the global GPS coordinate frame (East, North, Up). These transformed points are then quantized and added to a global map which is implemented as an occupied voxel list. The various lattice quantizations are tested on the same data and the results presented in Section IV.

Various metrics for quantization on 6DOF data obtained from a skid steer loader operating an autonomous mission are presented in Table I.

C. Radial distribution of lattice points

Fig. 3 depicts the variation in lattice point distances from a reference lattice point for the lattices in question for cells of equal volume. This plot is best explained by reference to the familiar cubic lattice. Considering the neighbours of a cubic cell of a cubic lattice there are expected $3^3 - 1 = 26$ adjacent cubes. The nearest neighbours are those associated with the faces of the cube of which there are six. This is evident in

Fig. 3 which has six points at a distance of one. The next nearest adjacent cells are those which share an edge with the central cube. Consequently as expected there are twelve lattice points at the next distance. Finally there are those cubic cells that are adjacent by virtual of sharing a corner and these eight lattice points are also apparent at the end of the cubic curve in Fig. 3. This is in stark contrast to the FCC line on Fig. 3 with the adjacent lattice points terminating after twelve with all being equidistant. The Voronoi cell for FCC (rhombic dodecahedron) means that the structure packs such that all adjacent voxels are adjacent through a face and so this results in the 12 equidistant nearest neighbours. This is the only 3D lattice to achieve this ideal neighbour arrangement.

The implications of Fig. 3 are borne out in the distributions generated for Fig. 4. This figure plots the distribution of distances from a lattice point to arbitrary points selected at random from the volume of a single cell as well as those encompassed by adjacent voxels.

Fig. 4 highlights the reduction in quantization error of the lattices FCC, BCC and MCC for the distribution of points within a single lattice cell.

The expected cubic probability increase is observed initially for all lattices because the sample volume increases with the cube of the radius. For the cubic lattice this increase terminates at 0.5 when the sample volume is clipped by the Voronoi cube face. This is similar for the other lattices each terminating at a slightly different point as a result of the differing Voronoi cell geometries.

Also contained within Fig. 4 are the distributions (from random data) of point distances for points in adjacent cells for each lattice. These distributions illustrate the significant improvement of the alternative lattices over cubic lattices for approximating proximity.

IV. Results and Discussion

A. Properties of Single Scans

Fig. 5 contains the cumulative distribution curves for the distortion and total number of lattice point voxels listed after
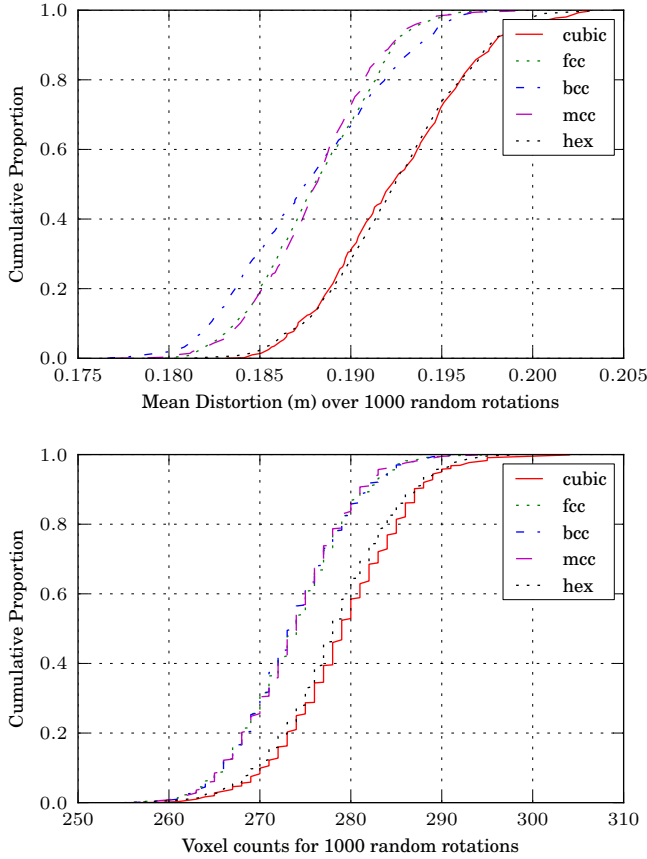
Fig. 5. Cumulative distribution curves for the quantization distortion and occupied voxel counts of 3D range scan data. The data are quantized to cubic, FCC, BCC, MCC and Hexagonal prismatic lattices of identical primitive unit cell volume.

quantization for various random rotations of the points of a single 3D range scan.

Although the cumulative frequency distortion curves in Fig. 5 are for real data the distortion is independent of whether the points are uniformly randomly distributed or distributed as the data of a real scan, if the data is randomly rotated. The errors introduced by quantization are clearly reduced by quantizing to the FCC and BCC lattices in preference to the cubic lattice as is apparent from the shift of the cumulative frequency curve to lower distortions.

When comparing the voxel counts in Fig. 5 it is apparent that although the lattice type makes only a slight difference to the voxel count for random data there is a larger improvement over the simple cubic lattice for real data for the FCC and BCC lattices. It is worth noting that although the BCC and FCC generally produce lower voxel counts in rare instances the cubic lattice is better. This is when the planar structures in the scan align with the coordinate axes. It is expected that this same effect is not present in the random data which has no such structure that benefits from coincidental alignment. Not only do these alternative lattices deliver lower voxel counts but also they deliver more consistent counts with reduced distortion.
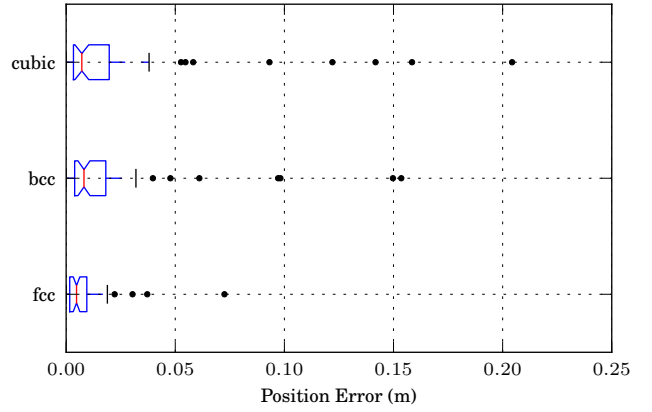

Fig. 6. Box plot of the scan matching position errors from 3D laser range data scans of an indoor environment. The whiskers are 1.5 times the interquartile range.

TABLE I

6DOF QUANTIZATION RESULTS FOR 3D MAPS TAKEN FROM A SKID STEER LOADER. 19399 LASER RANGE POINTS IN TOTAL WERE ADDED TO THE LATTICE MAP.

Lattice name	cell vol m^3	Voxel Count	MSE/ dimension	distance error (m)
cubic	0.125	3139	0.0226	0.2606
fcc	0.125	3197	0.0197	0.2432
bcc	0.125	3150	0.0195	0.2421
mcc	0.125	3078	0.0186	0.2365
hex	0.125	2904	0.0218	0.2560

B. Lattice Mapping Performance

For the lattice mapping experiments, scan matching is performed on real 3D laser data, acquired by a robot in an indoor office environment.

The relative pose between successive scans is determined via the multi-resolution occupied voxel list data structure and matching algorithm as described in [9]. The position errors are presented in Fig. 6 which indicates the lower position errors and better outlier performance for the FCC lattice over its cubic counterpart.

During the experiments it was noticed that cubic quantization can perform well in certain situations. For instance when the robot is travelling straight along a corridor the walls and floor are aligned with the robot's local coordinate frame and in this case cubic quantization is efficient. However the cubic lattice effectiveness is lost when the robot is not aligned with the corridor, is travelling on uneven ground or in less structured environments.

Various results for the lattices tested on data acquired from an autonomous skid steer loader are listed in Table I. In this case the MCC lattice performs the best with a low voxel count and lowest distance error per point.

V. CONCLUSION

The generic lattice quantization algorithm presented herein allows novel approaches, such as tuning or selection of the

lattice to a particular environment. For instance some environments might be suited to a hexagonal prismatic lattice due to their mostly planar nature and often uniform horizontal cross-section.

We established a generic algorithm feasible for low dimensions (≤ 3) quantization for the study of the performance of lattices of these dimensions. Quantization performance has been tested on both uniform data and field data collected from a mobile robotics platform.

Analysis of neighbours in the lattices is presented. A graph showing both the number of adjacent voxels and their centre distances is presented. Along with this are the lattice index deltas associated with these neighbouring voxels. These are necessary for many algorithms requiring proximity checks. The impact of these lattice adjacency patterns on uniformly sampled point data is also depicted, by plotting the distribution of point distances grouped by points in the same cell and those in the neighbouring cell volume. Knowing what voxels are adjacent and the probability distribution associated with their volumes are necessary steps towards path planning and collision checking on these lattices and are perhaps where the significant benefits to these lattices lie.

Both distortions (quantization error) and voxel counts are generally lower and more consistent with BCC, FCC and MCC quantization. Improvements in representation accuracy (minimal distortion) and reduction in voxel count are typically of the order of 5-10%. Another benefit is the ease with which the alternative lattice quantization process (Section II) can be combined with existing robotics algorithms and data structures such as occupancy grids, occupied voxel lists and ICP whilst still benefiting from superior quantisation accuracy as is evident in Fig. 6.

Finally, the FCC, BCC and MCC lattices are comparably better when compared to the equivalent cubic lattice. However, when considering the arrangement of adjacent cells, the FCC lattice is significantly superior to all other lattices. The adjacent cells in the FCC lattice, are fewer (12), equidistant and their volume has a tighter (40% smaller range) radial distribution.

A. Future Work

It is felt that the generic quantization algorithm for any lattice in low dimensions employed here has a number of opportunities for improvements in efficiency. The current algorithm relies on testing all 'off-by-one' lattice points. It is noticed that the actual off-by-one vectors are a subset of this for a particular lattice. Prediction of this subset, for example (4), given the lattice basis would accelerate quantization especially for higher dimensions (>3). Secondly the position of the point relative to the cell centre gives an indication of which proximate lattice points would need to be tested. Further optimisation approaches would also be sought.

The isodual nature of the MCC will be further investigated. This lattice is optimal in a number of measures and is comparable in accuracy to FCC and BCC.

As the gap in quantization performance between a cubic lattice and optimal lattices increases with dimensionality it would be interesting to test those optimal lattices in higher dimensions; higher dimensional data such as pose (6DOF) and image metrics. An example with pose would be determining whether a new pose is proximate to any pose in a previous history of poses. This is useful for detecting loop closure and for ensuring that only independent observations are added to the map. For real-time algorithms this query would have to be constant in time regardless of the number of historical poses. Such is possible with occupied voxels on various lattices. The more consistent distribution of nearest neighbours for the lattices is likely to improve the output of cell based path planning algorithms.

REFERENCES

[1] S. Thrun, "Learning occupancy grids with forward sensor models," *Autonomous Robots*, vol. 15, pp. 111–127, 2003.
[2] K. Konolige, "Improved occupancy grids for map building," *Autonomous Robots*, vol. 4, pp. 351–367, October 1997.
[3] A. Elfes, "Using occupancy grids for mobile robot perception and navigation," *Computer*, vol. 22(6), pp. 46–57, 1989.
[4] J. Ryde and H. Hu, "Mobile robot 3D perception and mapping with multi-resolution occupancy lists," in *Proceedings of IEEE International Conference on Mechatronics and Automation (ICMA 2007)*, Harbin, Heilongjiang, China, August 2007.
[5] E. S. Barnes and N. J. A. Sloane, "The optimal lattice quantizer in three dimensions," pp. 30–41, 1983.
[6] A. Gersho and R. M. Gray, *Vector Quantization and Signal Compression*. Kluwer Academic Publishing Group, 2001.
[7] J. H. Conway and N. J. A. Sloane, *Sphere Packing, Lattices and Groups*. Springer, 1999.
[8] S. D. Servetto, V. A. Vaishampayan, and N. J. A. Sloane, "Multiple description lattice vector quantization," *Proceedings 1999 Data Compression Conference*, pp. 13–22, 1999.
[9] J. Ryde and H. Hu, "3D mapping with multi-resolution occupied voxel lists," *Autonomous Robots*, vol. 28, no. 2, pp. 169–185, February 2010.
[10] J. Ryde and M. Brünig, "Non-cubic occupied voxel lists for robot maps," in *Proceedings of the IEEE/RSJ International Conference on Intelligent Robots and Systems (IROS)*, 2009.
[11] D. Micciancio, "The shortest vector problem is NP-hard to approximate to within some constant," *SIAM Journal on Computing*, vol. 30, no. 6, pp. 2008–2035, Mar. 2001, preliminary version in FOCS 1998.
[12] ——, "The hardness of the closest vector problem with preprocessing," *IEEE Transactions on Information Theory*, vol. 47, no. 3, pp. 1212–1215, 2001.
[13] D. Micciancio and S. Goldwasser, *Complexity of Lattice Problems: a cryptographic perspective*, ser. The Kluwer International Series in Engineering and Computer Science. Boston, Massachusetts: Kluwer Academic Publishers, Mar. 2002, vol. 671.
[14] J. Conway and N. Sloane, "Fast quantizing and decoding algorithms for lattice quantizers and codes," *IEEE Transactions on Information Theory*, vol. 28, pp. 227–232, 1982.
[15] ——, "A fast encoding method for lattice codes and quantizers," *IEEE Transactions on Information Theory*, vol. 29, pp. 820–824, 1983.
[16] J. H. Conway and N. J. A. Sloane, "The optimal isodual lattice quantizer in three dimensions," *Advances in Mathematics of Communication*, 2006.
[17] ——, "On lattices equivalent to their duals," *Journal Number Theory*, vol. 48, pp. 373–382, 1994.
[18] J. Arvo, *Fast random rotation matrices*. Academic Press, 1992, pp. 117–120.
[19] K. Shoemake, *Uniform random rotations*. Academic Press, 1992, pp. 124–132.
[20] R. Geraerts and M. H. Overmars, "Sampling techniques for probabilistic roadmap planners," 2003.
[21] A. Yershova and S. M. LaValle, "Deterministic sampling methods for spheres and SO(3)," in *Proceedings of the IEEE International Conference on Robotics and Automation (ICRA)*, 2004, pp. 3974–3980.
[22] S. R. Lindemann, A. Yershova, and S. M. Lavalle, "Incremental grid sampling strategies in robotics," in *In Proc. Workshop on Algorithmic Foundations of Robotics*, 2004, pp. 297–312.